

ORFEUS-II FAR-ULTRAVIOLET OBSERVATIONS OF 3C273: 1. INTERSTELLAR AND INTERGALACTIC ABSORPTION LINES¹

Mark Hurwitz, Immo Appenzeller², Juergen Barnstedt³, Stuart Bowyer, W. Van Dyke Dixon,
Michael Grewing³, Norbert Kappelman³, Gerhard Kraemer³, Joachim Krautter², and Holger Mandel²
Space Sciences Laboratory
University of California, Berkeley, California 94720-7450

ABSTRACT

We present the first intermediate-resolution ($\lambda / 3000$) spectrum of the bright quasi-stellar object 3C273 at wavelengths between 900 and 1200 Å. Observations were performed with the Berkeley spectrograph aboard the ORFEUS-II mission (Hurwitz et al. 1998). We detect Lyman β counterparts to intergalactic Lyman α features identified by Morris et al. (1991) at $cz = 19900, 1600, \text{ and } 1000 \text{ km s}^{-1}$; counterparts to other putative Lyman α clouds along the sight line are below our detection limit. The strengths of the two very low redshift Lyman β features, which are believed to arise in Virgo intracluster gas, exceed preflight expectations (Weymann et al. 1995), suggesting that the previous determination of the cloud parameters may underestimate the true column densities. A curve-of-growth analysis sets a minimum H I column density of $4 \times 10^{14} \text{ cm}^{-2}$ for the 1600 km s^{-1} cloud. We find marginally significant evidence for Galactic H₂ along the sight line, with a total column density of about 10^{15} cm^{-2} . We detect the stronger interstellar O VI doublet member unambiguously; the weaker member is blended with other features. If the Doppler b value for O VI is comparable to that determined for N V (Sembach, Savage, & Tripp 1997) then the O VI column density is $7 \pm 2 \times 10^{14} \text{ cm}^{-2}$, significantly above the only previous estimate (Davidsen 1993). The O VI/ N V ratio is about 10, consistent with the low end of the range observed in the disk (compilation of Hurwitz & Bowyer 1996). Additional interstellar species detected for the first time toward 3C273 (at modest statistical significance) include P II, Fe III, Ar I, and S III.

Subject headings: ISM: atoms, galaxies: clusters: individual: Virgo, quasars: individual: 3C273

1. OBSERVATIONS

We present the first intermediate-resolution far-ultraviolet spectrum of the bright quasi-stellar object 3C273 in the 900 – 1210 Å band, emphasizing absorption features arising along the line of sight. Appenzeller et al. (1998) discuss the intrinsic spectrum of 3C273. These data were collected with the Berkeley

¹Based on the development and utilization of ORFEUS (Orbiting and Retrievable Far and Extreme Ultraviolet Spectrometers), a collaboration of the Institute for Astronomy and Astrophysics of the University of Tübingen, the Space Astrophysics Group of the University of California at Berkeley, and the Landessternwarte Heidelberg.

²Landessternwarte, University of Heidelberg

³Institute for Astronomy and Astrophysics, University of Tübingen

spectrograph (Hurwitz et al. 1998) during the ORFEUS-SPAS II mission. The ORFEUS project and the *ASTRO-SPAS* platform are described in Grewing et al. (1991).

3C273 was observed five times, for a total of 10,797 s. All observations took place in late 1996, between 330/21:41 and 338/16:33 (Day of Year/HH:MM, GMT). The target coordinates were $\alpha = 12\ 29\ 06.7$, $\delta = +02\ 03\ 09$ (J2000). Absolute positioning of the 26'' diameter ORFEUS entrance aperture is accurate to $\pm 5''$. Extraction of the spectrum and subtraction of airglow follow the discussion in Hurwitz et al. (1998). Statistical and systematic uncertainties associated with background and airglow subtraction are properly tracked. As a final step, we bin the data on 0.1 Å centers.

In Figure 1 we show the complete spectrum (solid line), the 1σ uncertainty associated with shot noise and detector flat-field effects (dotted line), and a continuum established by an automated fitting routine (dashed line). The automated fitting routine identifies absorption features deeper than a statistically determined threshold, replaces those data with a linear interpolation from nearby wavelengths, smoothes heavily, then iterates twice more at increasing sensitivity to absorption lines. The resulting continuum has the advantage of being determined objectively, and evidently tracks most of the true spectrum well at wavelengths greater than 1000 Å. Like many such routines, however, this one yields unreliable results when strong features are closely spaced on a curved continuum (as in the region of absorption lines 3 and 4) and will tend to underestimate the true value when the spectrum contains a cluster of weak absorption features below the statistical threshold (note the weak dip in the fitted continuum around 1050 Å).

In Table 1 we list the interstellar absorption features and blends that are sufficiently strong and isolated for direct equivalent width measurement using the continuum shown in Figure 1 (unless otherwise noted). Statistical noise in the spectrum (1σ) corresponds to an unresolved absorption feature with equivalent width of about 0.040 Å; continuum placement uncertainty corresponds to about half that value. The value in the fourth column includes the statistical uncertainty only. For species whose column densities have not previously been reported, we list the minimum column (if optically thin) based on the best fit equivalent width and the oscillator strengths of Morton (1991).

The identification of most of the strong interstellar features listed in Table 1 is secure (Morton 1991). There are no obvious interstellar or intergalactic candidates for the unidentified line at 1008.5 Å, which may be spurious. Although the observed features at 1066.8 and 1048.2 Å presumably correspond to a pair of Ar I lines, their equivalent widths at first glance appear to be anomalous (the 1048.2 Å line should be stronger). As noted, however, the longer wavelength feature may be partially blended with an H₂ line at 1066.9 Å. The shorter wavelength feature probably suffers from local continuum depression by nearby H₂. Using the linear continuum shown in Figure 2, we estimate a best fit equivalent width closer to 0.13 Å. These systematic effects, in combination with the statistical errors, do much to reconcile the anomaly (especially if the features are on the flat part of the curve-of-growth).

Below 1000 Å, the increasing noise in the spectrum makes quantitative analysis of absorption features difficult, and the continuum fitting routine fails. Galactic features that are clearly detected include a blend from O I (and N III?) near 989 Å, C III (977.02 Å), Lyman δ (972.54 Å), and an N I blend near 953.8 Å. Higher series Lyman lines are likely to be filled in by diffuse emission (we correct for diffuse H I emission only through Lyman δ). An intriguing dip near 982 Å may be associated with C III in the Virgo cluster, but this identification is speculative. Difficulties in continuum placement render the equivalent widths very uncertain; we attempt no quantitative analysis of absorption lines below 1000 Å.

Table 1. Interstellar Lines and Equivalent Widths

#	W_{obs} (Å)	W_{eq} (Å)	σ (Å)	ID	$\text{Log } (N_{min})$ (cm ⁻²)
1	1206.44	0.573	0.056	Si III 1206.50	13.4
2	1199.75	0.896	0.114	N I blend	
3 ^a	1193.56	0.510	0.050	Si II 1193.29	
4 ^a	1190.58	0.532	0.051	Si II 1190.42	
5	1152.91	0.105	0.038	P II 1152.82	13.6
6	1144.92	0.340	0.054	Fe II 1144.94	
7	1143.44	0.137	0.040	Fe II 1143.22	
8	1134.63	1.135	0.084	N I blend	15.1
9	1122.54	0.157	0.038	Fe III 1122.53	14.3
10	1121.99	0.149	0.038	Fe II 1121.97	
11	1096.94	0.202	0.047	Fe II 1096.88	
12	1084.19	0.515	0.051	N II 1083.99, N II* blend	
13 ^b	1066.77	0.135	0.047	Ar I 1066.66	
14	1063.20	0.327	0.049	Fe II 1063.18 + H ₂	
15 ^c	1048.19	0.096	0.035	Ar I 1048.22	13.6
16	1039.18	0.433	0.044	O I 1039.23	
17	1031.87	0.363	0.038	O VI 1031.93	
18	1020.75	0.129	0.040	Si II 1020.70	
19	1012.53	0.083	0.036	S III 1012.50	14.4
20	1008.51	0.165	0.039	NOID	

^aContinuum determined with 2nd order local polynomial fit.

^bUp to 0.02 Å may be contributed by H₂ ($J = 2$).

^cContinuum may be depressed by adjacent weak lines.

2. INTERSTELLAR GAS

The equivalent widths of features at wavelengths of overlap with the bandpass of the Hubble Space Telescope are consistent with previous measurements from that instrument (Morris et al. 1991, Savage et al. 1993). For several other interstellar species (such as Fe II), parameters inferred from the GHRS measurements (Savage et al. 1993) yield predictions for lines in the ORFEUS band that are consistent with the features observed. Our spectrum represents the first detection of P II, Fe III, Ar I, and S III along this sight line. The statistical significance of these features is modest, as can be seen in Table 1. The minimum columns inferred for these elements (and for N I and Si III, features of which have been observed previously but whose column densities have not been reported) are shown in Table 1 and are of moderate interest only. Our minimum column for Fe III is a factor of 2.5 below that established for Fe II (Savage et al. 1993). The ratio of S III to S II (Savage et al. 1993) is at least 0.06 .

Interesting interstellar species unique to the ORFEUS band include H₂ and O VI, on which we now focus our attention. In Figure 2 we show a portion of the spectrum between 1046 and 1066 Å. This region is comparatively clear of competing interstellar lines and provides a convenient hunting ground for features of H₂. The solid line is the observed spectrum; the lowest dotted line is the 1 σ error. Overlying the data is a synthetic spectrum consisting of a flat continuum plus interstellar features convolved with the instrument response (dashed line). Wherever possible we adopt column densities, velocities, and effective Doppler b -values of atomic species from Savage et al. (1993). An atomic-only model (omitted for clarity) does not reproduce the observed modulation near 1050 Å nor the observed width of the the strong Fe II line at 1063.2 Å.

The total H₂ column density implied by our data is about $1 \times 10^{15} \text{ cm}^{-2}$, corresponding to a molecular fraction (f_{H_2}) of about 2×10^{-5} . This value is not exceptional for a low-reddening sight line (Shull & Beckwith 1982). The rotational excitation temperature T_{01} is poorly constrained but appears to be consistent with the range typical of interstellar clouds (50 – 80 K).

In Figure 3 we show a portion of the spectrum between 1023 and 1041 Å. The legend is as in Figure 2, except that we have not labeled a few weak features to avoid crowding. Features labeled Cld. 1 and Cld. 2 arise in intergalactic gas. The discrepancy between their synthetic and observed spectra is discussed below. The strong galactic Lyman β line is well fit in the wings; at the core, the subtraction of bright diffuse emission introduces a significant uncertainty indicated by the large peak in the error tracing. The stronger O VI doublet member (1031.9 Å) is resolved cleanly; the weaker member is blended but clearly present. To produce the fit shown in Figure 3, we found it necessary to set the column density of C II* near the upper limit from Savage et al. (1993). This modification to the C II* column does not significantly affect the previous determination that the cooling rate per nucleon is substantially below (about 1/6 of) the Galactic average (Savage et al. 1993).

With a b value of about 35 km s⁻¹ (estimated from the N V profile of Sembach, Savage, & Tripp 1997), our best estimate of the O VI column density is $7 \pm 2 \times 10^{14} \text{ cm}^{-2}$. Sembach, Savage, & Tripp (1997) found an N V column of $8 \times 10^{13} \text{ cm}^{-2}$, yielding an O VI/ N V ratio of about 10. The ratio along disk sight lines varies from about 10 to 20 (compilation of Hurwitz & Bowyer 1996). Ionization in this component of the hot galactic gas toward 3C273 therefore appears to be roughly similar to corresponding conditions in the disk. The fact that our measurement is near the low end of the disk range is qualitatively consistent with a scenario in which the gas is heated impulsively then cools as it moves away from the plane. Whether the comparatively high total column density is significantly nonrepresentative of the high latitude sky (Hurwitz & Bowyer 1996) will be determined with certainty only after study of many additional sight lines. The

presence of Radio Loops I and IV (Berkhuijsen, Haslam, & Salter 1971) cautions at the very least that division of our projected column by the midplane density (Jenkins 1978) should not be taken as a reliable estimate of the typical scale height. However, the fact that this first clear measurement of columns for both O VI and N V yields a value comparable to that in the disk bodes well for future far-ultraviolet missions such as FUSE. The previous measurement of O VI toward 3C273 (Davidsen 1993) had set only a lower limit on the column density, corresponding to an O VI/ N V ratio substantially below the range of disk values.

3. INTERGALACTIC GAS

Sixteen otherwise unidentified absorption features in the GHRS spectrum were attributed to intergalactic Lyman α clouds by Morris et al. (1991). Most of these are sufficiently weak that their higher Lyman series lines would not be detectable in our spectrum. We do find probable Lyman β counterparts to the strongest proposed Lyman α forest features, however. Morris et al. (1991) propose a cloud at $cz = 19900 \text{ km s}^{-1}$; from its column density and b value we predict a Lyman β equivalent width of 0.080 \AA at 1093.93 \AA . We find an otherwise unidentified feature within 0.2 \AA of the expected position with an equivalent width of $0.060 \pm 0.038 \text{ \AA}$ confirming, at least to 1.6σ , the intergalactic H I origin.

Of greater interest are a strong pair of features attributed to comparatively low redshift H I gas in the Virgo supercluster. Their Lyman α lines appear near $+1000$ and $+1600 \text{ km s}^{-1}$ (Weymann et al. 1995). Lyman β counterparts are expected at 1029.21 and 1031.16 \AA . We detect absorption features at 1029.11 and 1031.14 \AA ; however, the equivalent widths are stronger than expected. Weymann et al. (1995) employ profile fitting to constrain column densities and Doppler b values. Based on those parameters, the Lyman β equivalent widths are predicted to be 0.098 and 0.10 \AA , respectively. We observe $0.145 (\pm 0.037)$ and $0.241 (\pm 0.032) \text{ \AA}$. The disagreement is seen clearly in Figure 3, where the synthetic spectrum relies on the Weymann et al. (1995) parameters.

The discrepancy is particularly pronounced for the $+1600 \text{ km s}^{-1}$ cloud. Even with the parameters proposed by Weymann et al. the Lyman α line is saturated ($\tau_0 = 3.7$), so determination of a column density based solely on profile fitting of that feature may be affected by unresolved velocity structure and/or uncertainties in the instrumental profile. We have analyzed the GHRS spectrum to extract the equivalent width of the Lyman α line. In combination with the Lyman β line from the ORFEUS spectrum, we establish constraints on the logarithmic column density and effective b value for the $+1600 \text{ km s}^{-1}$ cloud using a curve-of-growth technique. We show the results, and the parameters proposed by Weymann et al., in Figure 4. Our results suggest that if the feature arises in a single cloud, its column density is higher by at least a factor of four compared to the value suggested by Weymann et al.. The curve-of-growth results are consistent with b values as low as 12 km s^{-1} and column densities in excess of 10^{18} cm^{-2} . Although this extremum of parameter space is probably inconsistent with the Lyman α profile fitting, it is not difficult to construct a multiple-cloud system that closely approximates the theoretical Voigt profile inferred from the Weymann et al. parameters while hiding a great deal of gas in the saturated core.

van Gorkom et al. (1993) searched for 21 cm emission from Virgo gas near the velocities of the absorbing clouds, detecting no H I to a limit of about $2.8 \times 10^{19} \text{ cm}^{-2}$. By adopting a relationship between the volume density of clouds with columns near the radio limit and of clouds with columns near those of the absorption line systems (Tytler 1987), the radio survey constrains the minimum size of the absorbing systems. The minimum permitted cloud size grows slowly with column density ($r_{cloud} \propto N^{0.25}$), so our results increase the minimum cloud size from about 4 kpc (van Gorkom et al. 1993) only to about 6 kpc, at

least for the smallest columns within our 95% confidence interval.

Other interstellar species that might conceivably be blended with the $+1600 \text{ km s}^{-1}$ cloud include Cl I at 1030.88 \AA , or H_2 ($J = 3$) at 1030.89 \AA . Based on the nondetection of other features from these species, we conservatively limit the equivalent width of their combined contribution to no more than 0.050 \AA . A contribution from Galactic O VI at high negative velocity is more difficult to rule out formally from our spectrum. Neither N V nor C IV appears at high negative velocity, however (Sembach, Savage, & Tripp 1997).

4. CONCLUSIONS

We observed the bright quasi-stellar object 3C273 for 10,797 s with the Berkeley spectrograph aboard the ORFEUS-II mission (Hurwitz et al. 1998). The resulting spectrum offers intermediate spectral resolution ($\lambda / 3000 \text{ FWHM}$) and a 1σ noise corresponding to an absorption feature with equivalent width of about 0.040 \AA .

The spectrum reveals, at modest statistical significance, a variety of previously undetected low ionization interstellar species, including P II, Fe III, Ar I, and S III. There is marginally significant evidence for H_2 , with a total column density of about 10^{15} cm^{-2} . The $J = 0$ and $J = 1$ rotational levels seem comparably populated, consistent with an excitation temperature T_{01} typical for interstellar clouds ($50 - 80 \text{ K}$).

We detect the stronger interstellar O VI doublet member unambiguously; the weaker member is blended. If the Doppler b value for O VI is comparable to that determined for N V (Sembach, Savage, & Tripp 1997), the O VI column density is $7 \pm 2 \times 10^{14} \text{ cm}^{-2}$. The O VI/ N V ratio is about 10, consistent with the low end of the range observed in the disk (compilation of Hurwitz & Bowyer 1996). If impulsively heated gas cools as it moves away from the Galactic disk, the O VI/ N V ratio might be expected to decrease (compared to the disk value) along halo sight lines.

We detect Lyman β counterparts to intergalactic Lyman α features identified by Morris et al. (1991) at $cz = 19900, 1600, \text{ and } 1000 \text{ km s}^{-1}$. Counterparts to other putative Lyman α clouds along the sight line are below our detection limit. The strengths of the two very low redshift Lyman β features, which are believed to arise in Virgo intracluster gas, exceed preflight expectations (Weymann et al. 1995). A curve-of-growth analysis sets a minimum H I column density of $4 \times 10^{14} \text{ cm}^{-2}$ for the 1600 km s^{-1} cloud. Following van Gorkom et al. (1993), our revised column density and nondetection of 21 cm radio emission discussed in that work can set a lower limit of about 6 kpc to the size of the Virgo cluster clouds.

We acknowledge our colleagues on the ORFEUS team and the many NASA and DARA personnel who helped make the ORFEUS-II mission successful. This work is supported by NASA grant NAG5-696.

REFERENCES

- Appenzeller, I., et al. 1998, ApJ
- Berkhuijsen, E. M., Haslam, C. G. T., & Salter, C. J. 1971, A&A, 14, 252
- Davidson, A. F. 1993, Sci., 259, 327
- Grewing, M., et al. 1991, in Extreme Ultraviolet Astronomy, ed. R. F. Malina & S. Bowyer (Elmsford: Pergamon), 437
- Hurwitz, M., & Bowyer, S. 1996, ApJ, 465, 296
- Hurwitz, M., et al. 1998, ApJ
- Jenkins, E. B. 1978, ApJ, 219, 845
- Morris, S. L., Weymann, R. J., Savage, B. D., & Gilliland, R. L. 1991, ApJ, 377, 21
- Morton, D. C. 1991, ApJS, 77, 119
- Savage, B. D., Lu, L., Weymann, R. J., Morris, S. L., & Gilliland, R. L. 1993, ApJ, 404, 124
- Sembach, K., Savage, B., & Tripp, T. M. 1997, ApJ, 480, 216
- Shull, M., & Beckwith, S. 1982, ARAA, 20, 163
- Tytler, D. 1987, ApJ, 321, 49
- van Gorkom, J. H., Bahcall, J. N., Jannuzi, B. T., & Schneider, D. P. 1993, A&A, 106, 2213
- Weymann, R. J., Rauch, M., Williams, R., Morris, S., & Heap, S. 1995, ApJ, 438, 650

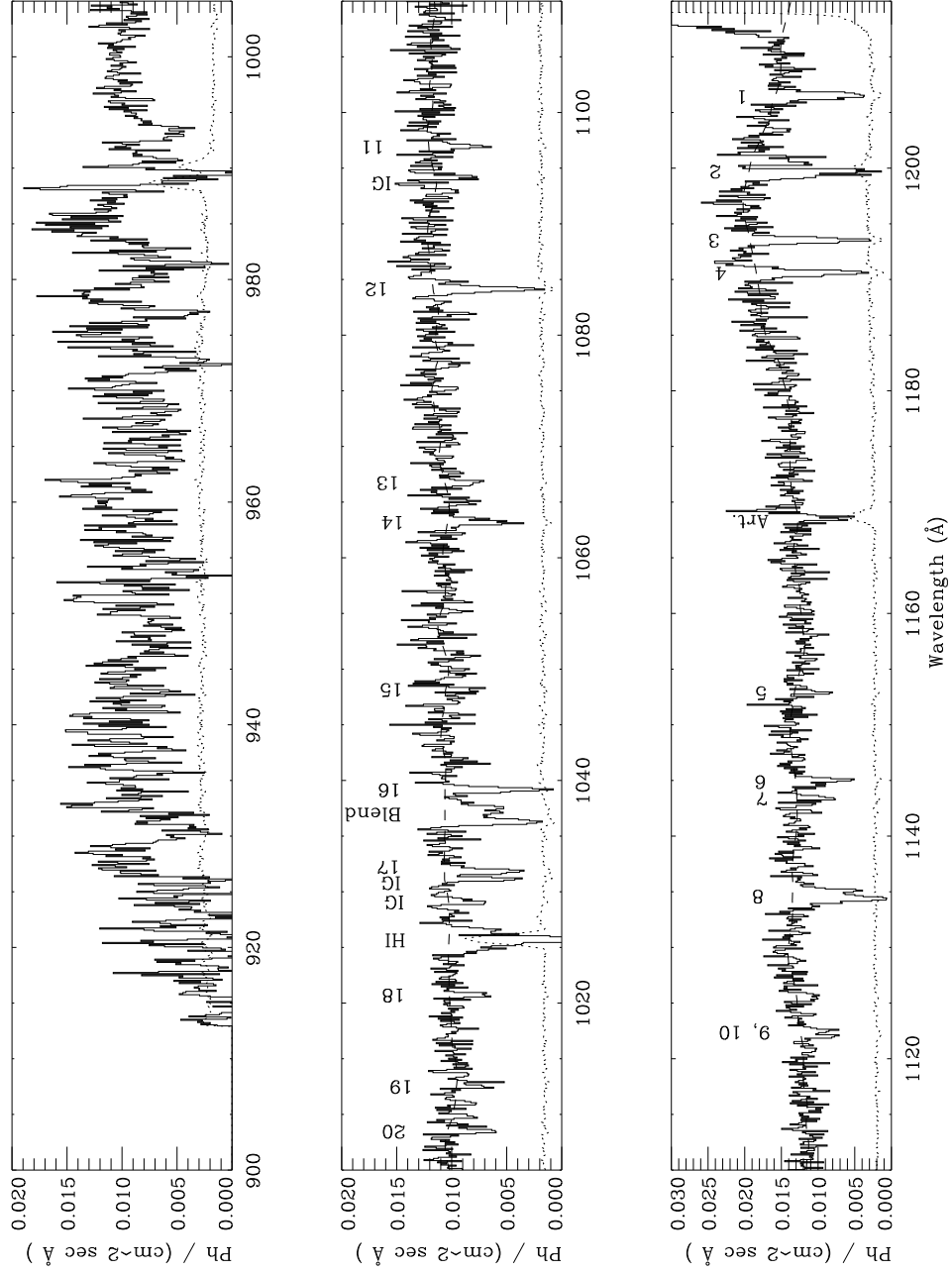


Fig. 1.— Observed spectrum of 3C 273 (solid line), 1σ uncertainty (dotted line), continuum fit longward of 1000 Å (dashed line). Numbered interstellar absorption features are identified in Table 1. The modulation near 1069 Å is an artifact associated with second-order He I diffuse emission. “IG” indicates intergalactic Lyman β features.

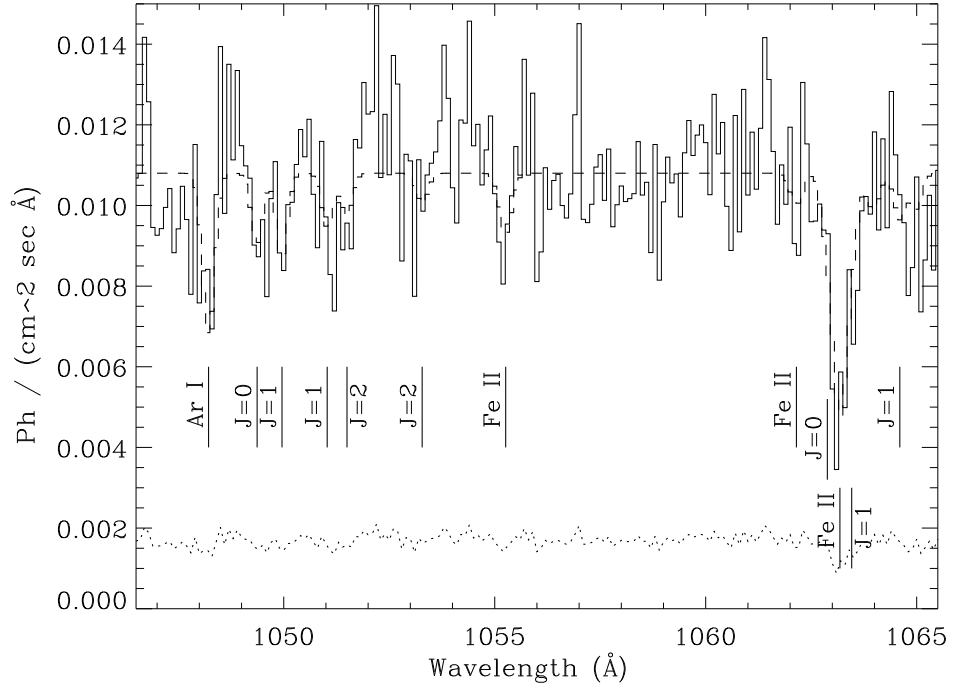


Fig. 2.— Observed spectrum of 3C 273 (solid line) with 1σ uncertainty (lower dotted line). Synthetic spectra overlying the data are based on a flat continuum plus interstellar atomic and H_2 features (dashed line). H_2 features are labeled with J level of lower state.

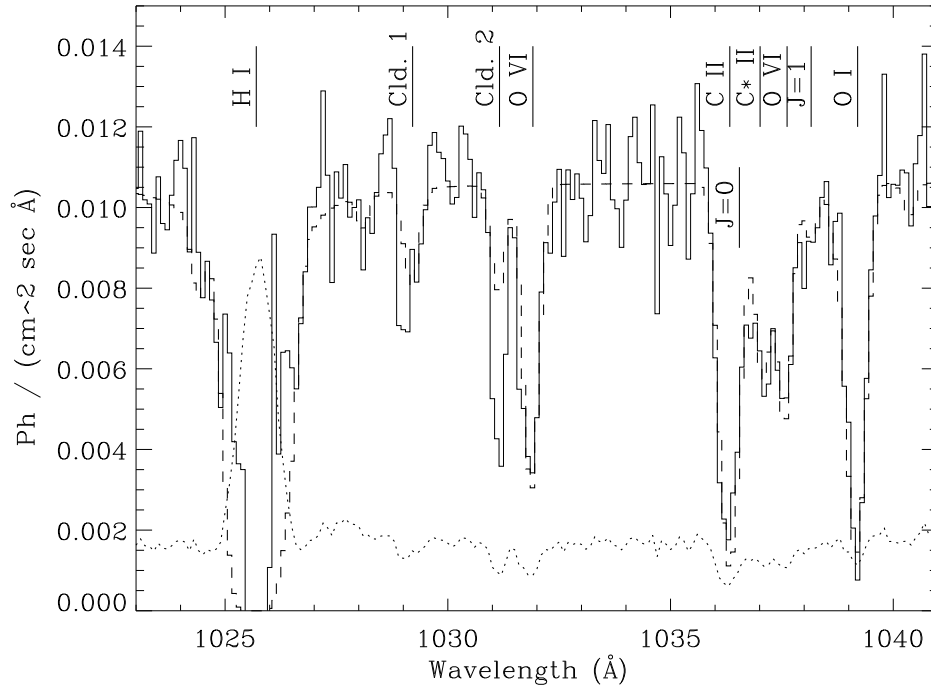


Fig. 3.— Observed spectrum of 3C 273 (solid line) with 1σ uncertainty (dotted line). Synthetic spectrum overlying the data is based on a flat continuum plus interstellar atomic and H_2 features and intergalactic features. H_2 features are labeled with J level of lower state. Features labeled “Cld. 1” and “Cld. 2” are Lyman β clouds in the Virgo cluster.

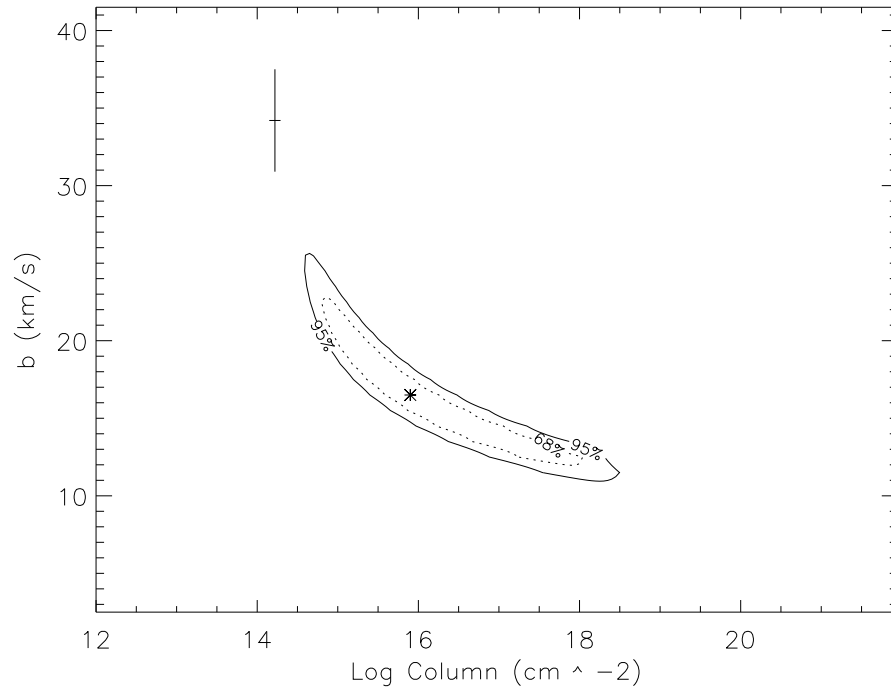


Fig. 4.— Constraints on logarithmic column density and effective Doppler b value for the 1600 km s^{-1} H I cloud. The cross centered at (14.22, 34) is based on Lyman α profile fitting (Weymann et al. 1995). The best-fit, 68% and 95% confidence intervals based on the equivalent widths of Lyman α (GHRS) and β (ORFEUS) are also shown.